

Charge and spin excitation spectra in the one-dimensional Hubbard model with next-nearest-neighbor hopping

S. Nishimoto,^{1,*} T. Shirakawa,² and Y. Ohta^{2,3}¹*Max-Planck-Institut für Physik Komplexer Systeme, D-01187 Dresden, Germany*²*Graduate School of Science and Technology, Chiba University, Chiba 263-8522, Japan*³*Department of Physics, Chiba University, Chiba 263-8522, Japan*

(Received 24 January 2007; published 4 March 2008)

We calculate spin and charge excitation spectra of the one-dimensional (1D) quarter-filled Hubbard model with nearest-neighbor t and next-nearest-neighbor t' hopping integrals using the dynamical density-matrix renormalization group technique. We consider a case where t (>0) is much smaller than t' (>0). First, we examine the accuracy of our method based on comparison between our result and exact noninteracting spectrum. Next, we investigate the spectra with the on-site Coulomb interaction. We find that the spin and charge excitation spectra are essentially the same as those of the 1D quarter-filled Hubbard (and t - J) model for the two 1D chains along the hopping integral t' . However, the hopping integral t ($<t'$) plays a crucial role in the short-range correlations and low-energy excitations; ferromagnetic correlation between electrons on neighboring sites is enhanced and pairing correlation between the electrons is induced. Consequently, a spin-triplet superconducting state may be derived.

DOI: [10.1103/PhysRevB.77.115102](https://doi.org/10.1103/PhysRevB.77.115102)

PACS number(s): 71.10.Pm, 71.10.Fd, 78.30.Jw, 72.15.Nj

I. INTRODUCTION

Spin-triplet superconductivity has been one of the major issues in the field of condensed matter physics. Nearly all the conventional and unconventional superconductors known to date are spin-singlet paired. The best-known example of triplet pairing is not a superconductor but a superfluid,³ He, where the atomic Cooper pairs are formed in spin-triplet channel.¹ Only a few materials of spin-triplet superconductivity have, so far, been confirmed in the strongly correlated electron systems; for example, the ruthenium-oxide Sr_2RuO_4 ,² sodium cobalt oxide bilayer-hydrate $\text{Na}_x\text{CoO}_2 \cdot y\text{H}_2\text{O}$,³ and heavy-fermion compounds such as UPt_3 .⁴ Here, some questions will naturally arise. One is whether the electron correlation can take an essential part in superconductivity carried by spin-triplet pairs. Another is how the behavior differs from that of spin-singlet superconductivity. In this manner, research on spin-triplet superconductivity might offer an opportunity to expose unknown physical phenomena.

Quite recently, a new mechanism of the spin-triplet superconductivity has been proposed in a fairly simple correlated system using the density-matrix renormalization group (DMRG) method.⁵ The model consists of two Hubbard chains coupled with zigzag bonds and has a unique structure of hopping integrals: sign of the hopping integrals changes alternately along the zigzag bonds connecting two chains, while the sign along the one-dimensional (1D) chain is always negative (a model where all the hopping integrals are taken to be positive is equivalent under canonical transformation). Under this sign rule of the hopping integrals, the ring-exchange mechanism yields ferromagnetic spin correlations; accordingly, attractive interaction between electrons is derived. Also, other DMRG studies⁶⁻⁸ have been carried out from an interest in ferromagnetism. They suggested that the spin gap vanishes for large interaction in contrast to a weak-coupling analysis⁹ which leads to only a spin-singlet super-

conducting state. In all the previous DMRG studies, the arguments were developed on the basis of only the static properties such as pair binding energy, spin excitation gap, and pairing correlation function, as well as spin-spin correlation function. Therefore, further investigations including dynamical properties must be needed.

The model may be of possible relevance to superconductivity observed in quasi-1D organic conductor (TMTSF)₂X [$X=\text{PF}_6, \text{ClO}_4$], which is the so-called Bechgaard salts.^{10,11} It exhibits a rich phase diagram upon variation of the pressure and the temperature. At low temperature, the phase changes in the order corresponding to spin-Peierls insulator, antiferromagnetic insulator, spin-density-wave (SDW) insulator, superconductivity, and paramagnetic metal, with an increase in the pressure. So far, experimental evidence that the superconducting state is in the triplet channel has been piled up.¹² However, physics of the spin-triplet superconductivity is less well understood. A newly synthesized copper-oxide compound $\text{Pr}_2\text{Ba}_4\text{Cu}_7\text{O}_{15-\delta}$ (Ref. 13) may also be a relating system. This material consists of single CuO chains (as in $\text{PrBa}_2\text{Cu}_3\text{O}_7$) and double CuO chains (as in $\text{PrBa}_2\text{Cu}_4\text{O}_8$), and those chains are separated by insulating CuO_2 plains. It has been reported that the double chains turn into a superconducting state below $T_c \sim 10$ K.¹⁴ The structure of the double CuO chains bears a certain similarity to our model.¹⁵

The purpose of the present study is to build up understanding of the low-energy physics of the 1D Hubbard model with positive nearest-neighbor hopping integral by calculating dynamical quantities. Due to the spin-charge separation, the spin and charge degrees of freedom must be dealt with separately. So we calculate the momentum-dependent dynamical spin-spin and density-density correlation functions using the dynamical density-matrix renormalization group (DDMRG) method,¹⁶ which is an extension of the standard DMRG method¹⁷ for calculating dynamical quantities. The obtained results with high resolution enable us to discuss the details of fundamental properties on the spin and charge ex-

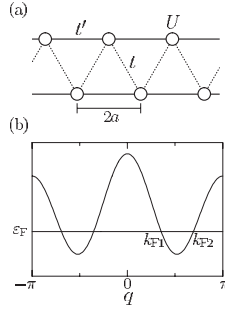


FIG. 1. (a) Lattice structure and (b) noninteracting band dispersion for $t'/t > 1$. The lattice constant a is defined as an intersite distance along the t chain.

citations. Thus, we can find some interesting features in the low-energy physics; they lead to the enhancement of ferromagnetic correlation between neighboring sites and the appearance of attractive interaction between electrons. As a result, a spin-triplet superconducting state may be derived. We are also confident that this investigation should provide deeper insight into the knowledge of ferromagnetism and spin-triplet superconductivity.

Our paper is organized as follows. In Sec. II, we define the 1D t - t' - U model and introduce the physical quantities of interest, namely, spin and charge excitation spectra. In Sec. III, exact solution of the spin (and charge) excitation spectrum in the noninteracting case is presented, and by comparing our result with them, we evaluate the performance of the DDMRG method. We then study the spectra with the on-site Coulomb interaction and discuss the relevance to the spin-triplet superconductivity. We close with a short summary in Sec. IV.

II. MODEL AND METHOD

We consider the 1D Hubbard model with next-nearest-neighbor hopping, the Hamiltonian is written as

$$H = t \sum_{i,\sigma} (c_{i+1\sigma}^\dagger c_{i\sigma} + \text{H.c.}) + t' \sum_{i,\sigma} (c_{i+2\sigma}^\dagger c_{i\sigma} + \text{H.c.}) + U \sum_i n_{i\uparrow} n_{i\downarrow}, \quad (1)$$

where $c_{i\sigma}^\dagger$ ($c_{i\sigma}$) is the creation (annihilation) operator of an electron with spin σ at site i and $n_{i\sigma} = c_{i\sigma}^\dagger c_{i\sigma}$ is the number operator. Here, t (>0) is the nearest-neighbor and t' (>0) the next-nearest-neighbor hopping integrals and U is the on-site Coulomb interaction [see Fig. 1(a)]. We call a chain along the t (t') hopping integral t chain (t' chain). The dispersion relation is given by

$$\varepsilon_k = 2t \cos ka + 2t' \cos 2ka, \quad (2)$$

where a is the lattice constant along the t chain (we set $a = 1$ hereafter). For $t'/t > (\cos^2[(2-\rho)\pi/2])/\sin^2[(2-\rho)\pi]$ (ρ is the band filling), there are two branches, namely, four Fermi momenta $\pm k_{F1}$ and $\pm k_{F2}$ ($|k_{F2}| > |k_{F1}|$), of the noninteracting Fermi surface [see Fig. 1(b)]. In this paper, we

restrict ourselves to the case where t' is a few times as large as t and the system is quarter filled, $\rho = 1/2$. Hence, the model can be regarded as a double t' -chain Hubbard model weakly coupled by t chain.

Because t is much smaller than t' , it would be very useful to allow a case of $t=0$ for familiarization with our results. In the limit of $t \rightarrow 0$, the system is equivalent to two independent 1D quarter-filled Hubbard chains since all electrons are distributed equally to the chains. The Brillouin zone is now folded in half and the noninteracting dispersion relation is $\varepsilon_k = 2t' \cos q$. There are two Fermi momenta, $\pm k_F^*$ ($=\pi/4$).

In order to study the correlation effect on the spin and charge degrees of freedom, we calculate the spin excitation spectrum,

$$S(q, \omega) = \frac{1}{\pi} \text{Im} \langle \Psi_0 | s_q^+ \frac{1}{\hat{H} + \omega - E_0 - i\eta} s_{-q}^- | \Psi_0 \rangle, \quad (3)$$

with $s_q^+ = (1/\sqrt{L}) \sum_r e^{iqr} c_{r\uparrow}^\dagger c_{r\downarrow}$, and charge excitation spectrum,

$$N(q, \omega) = \frac{1}{\pi} \text{Im} \langle \Psi_0 | n_q \frac{1}{\hat{H} + \omega - E_0 - i\eta} n_{-q} | \Psi_0 \rangle, \quad (4)$$

with $n_q = (1/\sqrt{L}) \sum_{r\sigma} e^{iqr} n_{r\sigma}$. Here, $|\Psi_0\rangle$ and E_0 are the ground-state wave function and energy of Hamiltonian (1). The DDMRG technique is applied to calculate the excitation spectra. We here use open-end boundary conditions (OBCs) for accurate calculation, because the system is relatively hard to deal with by the DMRG method due to large long-range hopping integrals.¹⁷ When the OBCs is used, we need to use the quasimomenta $k = \pi m / (L+1)$ for integers $1 \leq m \leq L$ on a chain with L sites to express the momentum-dependent operators s_q^+ and n_q .¹⁸

III. RESULTS

A. Noninteracting spectrum

First, let us consider the noninteracting case, $U=0$, where the model is exactly solvable. Then, since an excitation just corresponds for creating a particle-hole pair for the ground state, we can obtain the exact spectrum of spin excitations,

$$S(q, \omega) = \lim_{\eta \rightarrow 0} \frac{1}{L\pi} \sum_{\varepsilon_k < \varepsilon_F < \varepsilon_{k+q}} \frac{\eta}{(\omega - \varepsilon_{k+q} + \varepsilon_k)^2 + \eta^2}, \quad (5)$$

where small η is introduced to regularize the poles at particular frequency ω . Note that the spectrum of charge excitations is exactly twice as large as that of the spin excitation, i.e., $N(q, \omega) = 2S(q, \omega)$, for $U=0$, because $N(q, \omega)$ is just summed over both up and down spins.

In Fig. 2, we show the exact noninteracting spin excitation spectrum $S(q, \omega)$ [Eq. (5)]. For small $t/t' (< 1)$, the spectrum contains two predominant features: (i) large-weighted double sine curve structure whose dispersions are approximately written as $\omega \sim (4t' \pm 2t) \sin q$ and (ii) small-weighted continuum structure in low-frequency range, which arises from excitations between the different branches. A zero-energy excitation is caused by creation of a particle-hole pair just at the Fermi level ε_F , so that the gap closes at

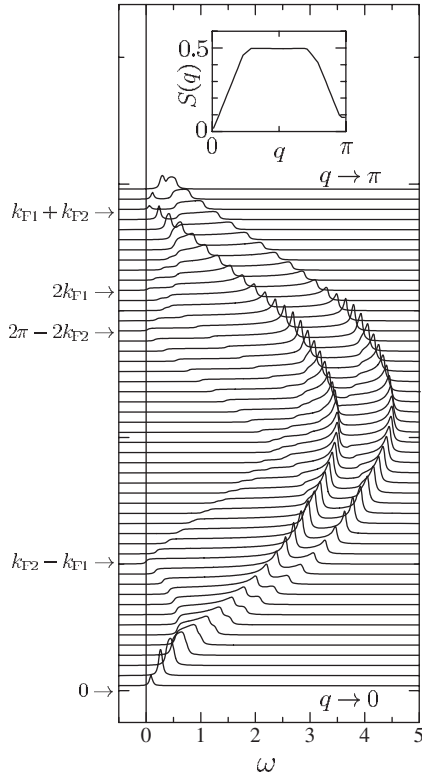


FIG. 2. Exact spin excitation spectrum $2S(q, \omega)$ [$=N(q, \omega)$] for $t=0.25$ and $t'=1$ in the noninteracting case ($U=0$). Broadening $\eta=0.03$ is introduced. Five momenta with arrow in the left side denote gapless points.

five momenta $q=0$, $k_{F2}-k_{F1}(=\pi/4)$, $2k_{F1}$, $2k_{F2}$, and $k_{F1}+k_{F2}$.

Now, we attempt to reproduce the noninteracting spin excitation spectrum (see Fig. 2) using the DDMRG method. Since the noninteracting model poses a nontrivial problem to the DDMRG technique, it gives us a relevant accuracy test. When carrying out the DDMRG calculation, one of the most important things is to take account of required CPU time. Ordinarily, the DDMRG method takes much longer time than the standard DMRG method because the excited states must be obtained and an asked quantity must be calculated (almost) individually for each frequency. Additionally, a required CPU time τ_{CPU} increases rapidly with frequency ω and/or system size L in the DDMRG calculation. It is estimated approximately as $\tau_{\text{CPU}} \propto \omega^\alpha (1 < \alpha < 2)$ and $\tau_{\text{CPU}} \propto L$, keeping the other conditions. Hence, it would be efficient to take a relatively small system for obtaining an overview of spectrum and larger system for studying a detailed structure in low-frequency range.

Let us then check our DDMRG result with the exact spectrum. In the right panel of Fig. 3, we show the spin excitation spectrum $S(q, \omega)$ for $U=0$ calculated with the DDMRG method in a chain with $L=24$ sites. The double sine curve structure can be clearly seen. However, it is hard to investigate dispersive structures in the low-frequency range because only discrete peaks can be obtained instead of the exact continuum spectra due to finite-size effect. We need to take larger system to resolve this problem since the resolution of

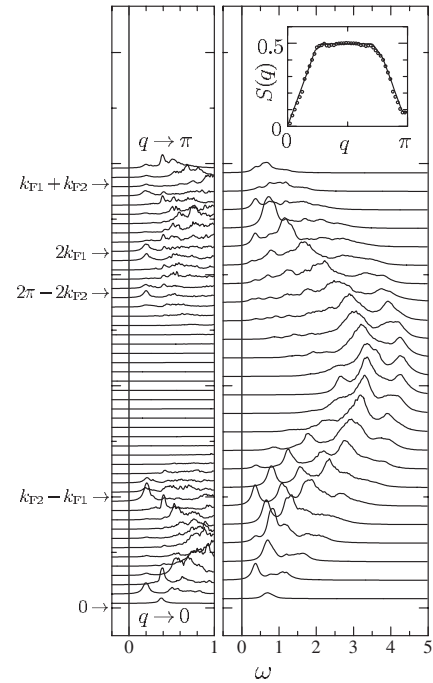


FIG. 3. Spin excitation spectrum $2S(q, \omega)$ [$=N(q, \omega)$] for the same parameter set as Fig. 2 in the noninteracting case ($U=0$) calculated with the DDMRG method. Right (left) panel is result for $L=24$ and $\eta=0.1$ ($L=48$ and $\eta=0.04$). Inset: spin structure factor $S(q)$ obtained from ω integration of $S(q, \omega)$.

spectrum can be improved in proportion to the system size. We therefore choose to double the system size, $L=48$, and consider the low-energy excitations. The result is shown in the left panel of Fig. 3. The resolution is obviously improved, and we can now confirm the five momenta which should give zero excitation. Moreover, we can see good agreement of the spin structure factor $S(q)$ [$=\sum_\omega S(q, \omega)$] between the DDMRG and the exact results, as shown in the inset of Fig. 3. Thus, we are confident that the DDMRG method, indeed, enables us to study the details of relatively complicated spectrum structures.

For the information, we keep $m=400$ (800) density-matrix eigenstates to obtain the spectrum for $L=24$ (48) sites. Note that a larger m value would be necessary to get the “correct” ground state and excited state $s_{-q}^-|\Psi_0\rangle$ (or $n_{-q}|\Psi_0\rangle$) of the system. Actually, we set $m=1200$ in the first four to five DDMRG sweeps.

B. Spin excitation spectrum

Next, we see how the spin excitations is changed with the on-site Coulomb interaction. Figure 4 shows the spin excitation spectrum $S(q, \omega)$ for $t=0.25$, $t'=1$, and $U=10$ calculated with the DDMRG in a chain with $L=24$ (right panel) and with $L=48$ (left panel). Roughly speaking, the lower edge of the spectrum consists of three sine curves with four nodes: $q \sim 0$, $k_{F2}-k_{F1}(=\pi/4)$, $\pi-(k_{F2}-k_{F1})(=3\pi/4)$, and π . The excitation gap seems to close around these nodes. It is consistent with previous theoretical studies,^{5,7} which have suggested that no spin gap exists in the strong-coupling regime.

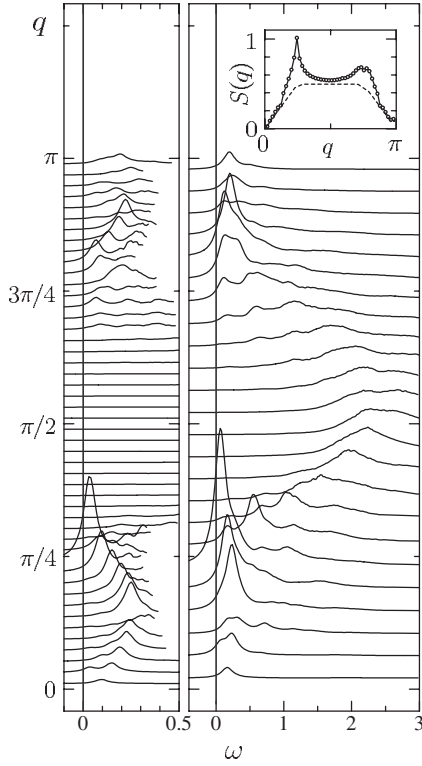


FIG. 4. Spin excitation spectrum $S(q, \omega)$ in $t=0.25$, $t'=1$, and $U=10$ calculated with the DDMRG method for $L=24$, $\eta=0.1$ (right panel) and $L=48$, $\eta=0.04$ (left panel). Inset: spin structure factor $S(q)$ obtained from ω integration of $S(q, \omega)$.

On the other hand, the higher edge of the spectrum is approximately represented as a sine curve $\omega \sim \sin q$ as in the case of $U=0$, which comes from the creation of particle-hole pairs within the same branch.

Let us now take a closer look at the spectrum. As far as the spin degrees of freedom are concerned, model (1) for large U may be mapped into a two-chain t - J model coupled with zigzag bonds. For small t/t' , antiferromagnetic interaction along the t' chain, J' , must be much larger than that along the t chain, J , if we assume that the exchange interaction comes from the second-order perturbation of hopping integral with a fixed U , i.e., $J'(\sim t'^2) \gg J(\sim t^2)$. Consequently, the features of spectrum can be basically interpreted as those of the 1D quarter-filled t - J model.^{20–22} The nodes of lower edge in the DDMRG spectrum correspond to $q=0$, k_F^* , $\pi - k_F^*$, and π , respectively. Also, we can see considerable enlargement of spectral intensities around $q=\pi/4(=k_{F2}-k_{F1})$ as compared with the noninteracting spectrum. This means that the onsite Coulomb interaction enhances antiferromagnetic correlation with a period of four times the lattice constant along the t' chain, which can be easily expected from the fact that the $2k_F$ -SDW correlation is the most dominant for small J in the 1D quarter-filled t - J model. This result is compatible with the $2k_F$ -SDW state observed experimentally in $(\text{TMTSF})_2\text{X}$.¹⁹

We then study the effect of small hopping integral t , which leads to the antiferromagnetic interaction J along the t chain as mentioned above. From the viewpoint of the spin

degrees of freedom, magnetical frustration must be brought because triangular lattices are formed of only the antiferromagnetic interactions. Although J is much smaller than J' , we can clearly see the influence in the DDMRG spectrum; there are two nodes around $q=3\pi/4$: i.e., $q \sim 2k_{F1} (>3\pi/4)$ and $2\pi-2k_{F2} (<3\pi/4)$. These nodes are collected into a single node at $q=3\pi/4$ when $t=0$. This split actually signifies a tendency to a formation of $2k_F$ -SDW state along the t chain as well as to a collapse of $2k_F$ -SDW state along the t' chain. With increasing t/t' , the node at $q=2k_{F2}$ approaches $q=\pi/2$ and the adjacent spectral weight increases, whereas the node at $q=2k_{F1}$ goes away from $q=3\pi/4$ and the weight goes toward zero. In other words, the hopping term t weakens the $2k_F$ -SDW oscillation along the t' chain since the competing antiferromagnetic correlation along the t chain is enhanced. Hence, the spectral weight around $q=\pi/4$ will certainly diminish as t/t' increases.

Another noticeable feature is that spectral weight around $q=3\pi/4$ is obviously smaller than that around $q=\pi/4$, while the spectrum should be symmetrical about $q=\pi/2$ in the case of $t=0$. For clearer understanding, we study the spin structure factor $S(q)$. As shown in the inset of Fig. 4, it is evident that $S(q)$ around $q=\pi/4$ is greater than that around $q=3\pi/4$; otherwise, $S(q)$ seems to be almost symmetrical to $q=\pi/2$. This implies an enhancement of ferromagnetic correlation between neighboring sites along the t chain, which is explained in the following paragraph. Note that, however, the ground state is not ferromagnetically polarized since the slope of $S(q)$ at $q=0$ is almost unchanged from the $U=0$ result.

A real-space behavior of the spin-spin correlation may be derived from the Fourier transform of $S(q)$,

$$\langle S_i^z S_j^z \rangle = \frac{1}{L} \sum_q S(q) e^{iq(r_i - r_j)}, \quad (6)$$

with $S_i^z = (n_{i\uparrow} - n_{i\downarrow})/2$. We find that the spin correlation along the t' chain could not be affected so much by small t , but the decay length of the $2k_F$ -SDW oscillation is slightly shortened. On the contrary, the t hopping term plays a prominent role in spin correlation between the t' chains. It is estimated as $\langle S_i^z S_{i+R}^z \rangle \propto \cos[(\pi/4)R] \times (\text{decaying term})$, where R is odd number. For $R=1$, $\langle S_i^z S_{i+1}^z \rangle = 0.00745$ is obtained, which indicates the presence of ferromagnetic correlation between two electrons at the neighboring sites. This result is consistent with a scenario of spin-triplet superconductivity where the pairing of electrons occurs between the inter- t' -chain nearest-neighbor sites, proposed in Ref. 5.

C. Charge excitation spectrum

Finally, we study the charge correlation function with the on-site Coulomb interaction. Figure 5 shows the charge excitation spectrum $N(q, \omega)$ for $t=0.25$, $t'=1$, and $U=10$, calculated with the DDMRG method in a chain with $L=24$ (right panel) and with $L=48$ (left panel). The outline of spectrum, which is roughly expressed as $\omega \approx 4t' \sin q$, seems to be similar to that in the noninteracting spectrum. This result reflects the fact that the dispersion is hardly affected by the

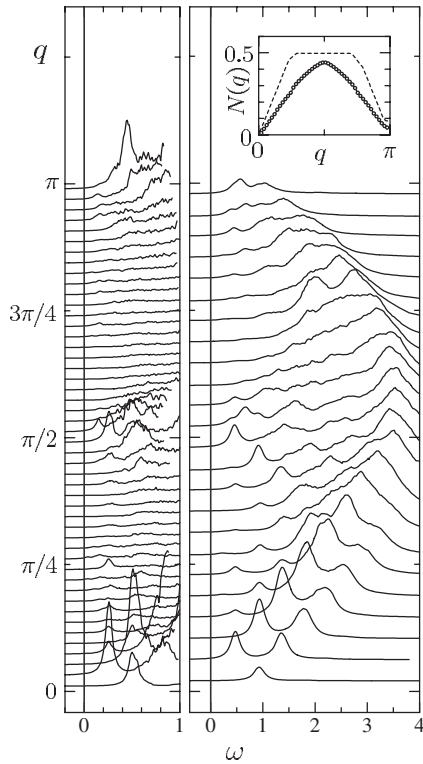


FIG. 5. Charge excitation spectrum $N(q, \omega)$ in the same parameter set as Fig. 4 calculated with the DDMRG method for $L=24$, $\eta=0.1$ (right panel) and $L=48$, $\eta=0.04$ (left panel). Inset: charge structure factor $N(q)$ obtained from ω integration of $N(q, \omega)$.

on-site Coulomb interaction. Instead, two distinctive features emerge in the low-frequency range as discussed below.

One is the increase of spectral weight around $q=\pi/2$ in the low-energy excitations. The excitation gap also seems to close there. Thus, lower edge of the spectrum consists of two sine curves with three nodes: $q\sim 0$, $\pi/2$, and π . This gives a tendency to the Peierls instability, namely, a formation of the $4k_F$ -charge-density wave (CDW) along the t' chain. It would be more evident if we look over the momentum-dependent charge structure factor $N(q)$, as shown in the inset of Fig. 5. It shows the maximum value at $q=\pi/2$ and practically the straight line up to $q=\pi/2$ from $q=0$ (or π). It is consistent with results in the 1D quarter-filled Hubbard chain.²³ In fact, this result is almost equivalent to a half-filled band of non-interacting spinless electrons as far as the charge degrees of freedom are concerned.

The other is an appearance of large-weighted sharp peaks around $q=0$ at $\omega\approx 0$. The point is as follows: spectral weight of the peaks around $q=0$ is larger than that around $q=\pi$ in the low-frequency range, and they are also gathered at lower frequencies. This implies that the electrons tend to come in the neighboring sites along the t chain, which is associated with pairing of two electrons between the inter- t' -chain sites; accordingly, the pairs tend to be arranged alternately along t'

chain. Note that momenta $q=0$ and π should be equivalent when $t=0$, so that the small hopping integral t enhances the pairing correlation. Additionally, we can estimate the so-called Luttinger parameter as K_ρ from the derivative of $N(q)$ at $q=0$, i.e., $K_\rho=(\pi/2)[dN(q)/dq]_{q=0}$; we thus find the value $K_\rho\approx 0.637$. The superconducting correlation can be the most dominant one since $K_\rho>0.5$ is the criterion in a model with four Fermi points.^{24,25} These results are also consistent with the spin-triplet superconducting mechanism proposed in Ref. 5.

IV. SUMMARY

In order to study the low-energy physics of the 1D Hubbard model with next-nearest-neighbor hopping integral, the spin and the charge excitation spectra are calculated using the DDMRG method. We first demonstrate the accuracy of the DDMRG method in comparison with the noninteracting exact spectrum. We suggest, for practical calculation, that it is necessary to take a relatively small system for obtaining an overview of spectrum and larger system for investigating detailed structures of low-frequency range because a required CPU time increases rapidly for higher frequency and/or larger system. Thus, the DDMRG method enables us to study the details of relatively complicated spectrum structures.

We then introduce the on-site Coulomb interaction. The spin and charge excitation spectra are essentially the same as that of the 1D quarter-filled Hubbard (and t - J) model; namely, the $2k_F$ -SDW and the $4k_F$ -CDW correlations along the hopping integral t' are enhanced. However, the hopping integral t , even if it is small, plays a crucial role for short-range correlations and low-energy physics; ferromagnetic correlation between electrons on neighboring sites is enhanced and pairing correlation between the electrons is induced. Consequently, our dynamical calculations support the spin-triplet superconducting mechanism where the pairing of electrons occurs between the inter- t' -chain nearest-neighbor sites.

Last, we mention a possible further extension of this work. We must obtain a strong evidence of the dominant spin triplet pairing state if the current spin-susceptibility could be successfully calculated. However, sufficiently accurate calculations are not simple and will require considerable efforts.

ACKNOWLEDGMENTS

We thank T. Takimoto, E. Jeckelmann, and H. Benthien for useful discussions. This work was supported in part by Grants-in-Aid for Scientific Research (Nos. 18028008, 18043006, and 18540338) from the Ministry of Education, Science, Sports, and Culture of Japan. A part of the computations was carried out at the Research Center for Computational Science, Okazaki Research Facilities, and the Institute for Solid State Physics, University of Tokyo.

- *Present address: Leibniz-Institut für Festkörper- und Werkstoffforschung Dresden, P.O. Box 270116, D-01171 Dresden, Germany.
- ¹A. J. Leggett, *Rev. Mod. Phys.* **47**, 331 (1975).
- ²Y. Maeno, H. Hashimoto, K. Yoshida, S. Nishizaki, T. Fujita, J. G. Bednorz, and F. Lichtenberg, *Nature (London)* **372**, 532 (1994).
- ³K. Takada, H. Sakurai, E. Takayama-Muromachi, F. Izumi, R. A. Dilanian, and T. Sasaki, *Nature (London)* **422**, 53 (2003).
- ⁴R. Joynt and L. Taillefer, *Rev. Mod. Phys.* **74**, 235 (2002).
- ⁵Y. Ohta, S. Nishimoto, T. Shirakawa, and Y. Yamaguchi, *Phys. Rev. B* **72**, 012503 (2005).
- ⁶R. Arita, K. Kuroki, H. Aoki, and M. Fabrizio, *Phys. Rev. B* **57**, 10324 (1998).
- ⁷S. Daul and R. M. Noack, *Phys. Rev. B* **58**, 2635 (1998).
- ⁸S. Nishimoto, T. Shirakawa, and Y. Ohta, arXiv:0710.2274v1 (unpublished).
- ⁹M. Fabrizio, *Phys. Rev. B* **54**, 10054 (1996).
- ¹⁰D. Jérôme, A. Mazaud, M. Ribault, and K. Bechgaard, *J. Phys. (France) Lett.* **41**, L95 (1980).
- ¹¹K. Bechgaard, K. Carneiro, M. Olsen, F. B. Rasmussen, and C. S. Jacobsen, *Phys. Rev. Lett.* **46**, 852 (1981).
- ¹²I. J. Lee, S. E. Brown, and J. Naughton, *J. Phys. Soc. Jpn.* **75**, 051011 (2006), and references therein.
- ¹³M. Matsukawa, Y. Yamada, M. Chiba, H. Ogasawara, T. Shibata, A. Matsushita, and Y. Takano, *Physica C* **411**, 101 (2004).
- ¹⁴S. Sasaki, S. Watanabe, Y. Yamada, F. Ishikawa, K. Fukuda, and S. Sekiya, arXiv:cond-mat/0603067 (unpublished).
- ¹⁵K. Sano, Y. Ōno, and Y. Yamada, *J. Phys. Soc. Jpn.* **74**, 2885 (2005).
- ¹⁶E. Jeckelmann, *Phys. Rev. B* **66**, 045114 (2002).
- ¹⁷S. R. White, *Phys. Rev. Lett.* **69**, 2863 (1992); *Phys. Rev. B* **48**, 10345 (1993).
- ¹⁸H. Benthien, F. Gebhard, and E. Jeckelmann, *Phys. Rev. Lett.* **92**, 256401 (2004).
- ¹⁹For a review article, see T. Ishiguro, K. Yamaji, and G. Saito, *Organic Superconductors* (Springer-Verlag, Berlin, 1990).
- ²⁰P. A. Bares and G. Blatter, *Phys. Rev. Lett.* **64**, 2567 (1990).
- ²¹T. Tohyama, P. Horsch, and S. Maekawa, *Phys. Rev. Lett.* **74**, 980 (1995).
- ²²Y. Saiga and Y. Kuramoto, *J. Phys. Soc. Jpn.* **68**, 3631 (1999).
- ²³J. E. Hirsch and D. J. Scalapino, *Phys. Rev. B* **27**, 7169 (1983).
- ²⁴N. Nagaosa, *Solid State Commun.* **94**, 495 (1995).
- ²⁵H. J. Schulz, *Phys. Rev. B* **53**, R2959 (1996); in *Correlated Fermions and Transport in Mesoscopic Systems*, edited by T. Martin, G. Montambaux, and T. Trân Thanh Vân (Editions Frontières, Gif-sur-Yvette, France, 1996), p. 81.